

- (4) Stejskal, E. D.; Schaefer, J. J. *Magn. Reson.* **1975**, *18*, 560.
- (5) Tegenfeldt, J.; Haeberlen, U. *J. Magn. Reson.* **1979**, *36*, 453.
- (6) VanderHart, D. L.; Earl, W. L.; Garroway, A. N. *J. Magn. Reson.* **1981**, *44*, 361.
- (7) Suwelack, D.; Rothwell, W. P.; Waugh, J. S. *J. Chem. Phys.* **1980**, *73*, 2559.
- (8) Rothwell, W. P.; Waugh, J. S. *J. Chem. Phys.* **1981**, *74*, 2721.
- (9) Look, D. C.; Lowe, I. J. *J. Chem. Phys.* **1966**, *44*, 3437.
- (10) Whittaker, E.; Watson, G. N. "Modern Analysis"; Cambridge University Press: Cambridge, 1946; p 328. Condon, E. U.; Shortley, G. H. "The Theory of Atomic Spectra"; Cambridge University Press: Cambridge, 1935; p 53.
- (11) Heijboer, J., Ph.D. Thesis, University of Leyden, 1972.
- (12) Slichter, W. P. *J. Polym. Sci. Part C* **1966**, *14*, 33.

## <sup>13</sup>C NMR Analysis of Microstructure in the Highly Piezoelectric Copolymer Vinylidene Cyanide-Vinyl Acetate

Yong Sung Jo, Yoshio Inoue, and Riichirô Chûjô\*

Department of Polymer Chemistry, Tokyo Institute of Technology, Meguro-ku, Tokyo 152, Japan

Kazuo Saito and Seizo Miyata

Department of Material Systems Engineering, Faculty of Technology, Tokyo University of Agriculture and Technology, Koganei-shi, Tokyo 184, Japan. Received December 28, 1984

**ABSTRACT:** The microstructure of vinylidene cyanide-vinyl acetate copolymer was studied by 125-MHz <sup>13</sup>C NMR spectroscopy. Compositional sequence distributions obtained from cyanide (VDCN-centered) and methyl (VAc-centered) triads were in good agreement with the predicted sequence distributions calculated by using the reactivity ratios ( $r_1$ ,  $r_2$ ) and the conditional probabilities for cross propagation ( $P_{12}$ ,  $P_{21}$ ). Configurational results in the alternating sequence were interpreted in terms of our defined  $\epsilon$ -enchainments (those of a group relative to the other separated by five skeletal carbons) assuming VAc-VDCN as a repeating unit.  $\epsilon$ -Isotacticity  $\sigma_\epsilon$  could be obtained from cyanide carbon resonance as well as from methine carbon resonance, showing good agreement with each other. It was found that vinylidene cyanide-vinyl acetate copolymer is a highly alternating copolymer with a nonstereoregular structure.

### Introduction

It is well-known that crystalline polymers having large dipole moments in the side chains can exhibit piezoelectric properties if the main chains have an all-trans conformation (planar zigzag structure) and if the crystal structure shows a spontaneous polarization. Poly(vinylidene fluoride) has received major attention in the polymorphism of the crystalline structure because its electrical properties are closely related to the crystalline structure.<sup>1,2</sup> Much interest has recently been also centered on the copolymer of vinylidene fluoride and trifluoroethylene. The conformations of the copolymer may be transformed into a well-ordered planar zigzag phase from a mixture of disordered trans-planar and 3/1-helical phases by mechanical or electrical treatments, resulting in a ferroelectric to paraelectric phase transition.<sup>3,4</sup>

Recently, we found fairly good piezoelectric activity in a copolymer of vinylidene cyanide and vinyl acetate (hereafter, an abbreviation is used: P(VDCN-VAc)). This copolymer, however, seems to be almost amorphous because no melting is observed by DSC and it has broad X-ray reflections at  $2\theta = 15^\circ$  and  $2\theta = 30^\circ$ .<sup>5</sup> Infrared absorption at  $2240\text{ cm}^{-1}$  corresponds to the stretching vibration of the C $\equiv$ N group. From the poling time dependence of the absorbance of this band the origin of the marked piezoelectric behavior is deduced to be the rotation of the C—C $\equiv$ N group, the dipole moment of which is 4.0 debye.<sup>6</sup> As reported in the previous paper,<sup>7</sup> there is another interesting phenomenon in P(VDCN-VAc). This is a noticeable enthalpy relaxation in the region of the glass-transition temperature ( $T_g$ ). By isothermal annealing below  $T_g$ , enthalpy relaxation toward the equilibrium glassy state appears whereas glasses usually exist in a nonequilibrium state.<sup>8</sup> For P(VDCN-VAc) structural changes during enthalpy relaxation correspond to molec-

ular motions relevant to the dipolar rotation of C—C $\equiv$ N groups. Therefore, during poling in a high dc electric field, the cyanide group is believed to orient to some extent also in the amorphous phase because of the existence of finite free volume.

The molecular structures of piezoelectric polymers have been considered as one of the most important factors in determining piezoelectric activity. Molecular conformation is especially important, as well as chain structure, in understanding the origin of piezoelectricity not only in crystalline but also in amorphous polymers. For crystalline poly(vinylidene fluoride), Douglass<sup>9,10</sup> and his co-workers have provided useful information on the macroscopic dipole orientation with respect to the poling direction by observing the NMR line-width anisotropy. Their NMR results are in agreement with those of X-ray studies. However, the origin of the piezoelectricity in amorphous polymers has not yet become fully understood because of the lack of structural information concerning the amorphous material.

Generally, high-resolution NMR spectroscopy has been the very effective means for the elucidation of the microstructure of synthetic polymers.<sup>11,12</sup> In the present work, <sup>13</sup>C high-resolution NMR spectra of a P(VDCN-VAc) sample have been obtained for the first time with spectrometers operating at 25 and 125 MHz. The higher field NMR spectrum has been particularly successful in providing detailed information on the monomer sequence distribution and the stereochemical configuration of P(VDCN-VAc) copolymer.

### Experimental Section

**Materials.** The vinylidene cyanide (VDCN) was prepared from bi(acetyl cyanide).<sup>13</sup> The copolymer of vinylidene cyanide and vinyl acetate (VAc) was synthesized by radical polymerization

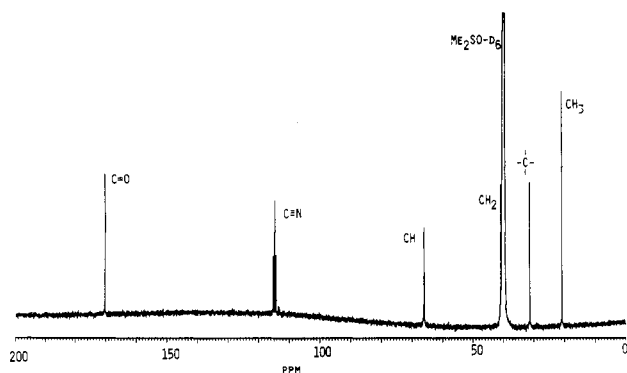


**Figure 1.** 125-MHz  $^{13}\text{C}$  NMR spectrum of vinylidene cyanide-vinyl acetate copolymer in  $\text{Me}_2\text{SO}-d_6$  at  $65^\circ\text{C}$ .

of VDCN and VAc with equal initial mole fractions. The copolymerization was initiated at  $45^\circ\text{C}$  in benzene by adding 0.2% (of total weight of monomers) *o,o'*-dichlorobenzoyl peroxide. On completion of the reaction, the copolymer began to coagulate and precipitate from a benzene solution. After the coagulum was washed with distilled benzene to remove any nonreactive monomer, the copolymer was dissolved in a few percent concentration of dimethylformamide. The solution was then poured gradually into benzene to reprecipitate for purification. The purified copolymer was then dried in a vacuum oven to constant weight.

Atactic poly(vinyl acetate), used for a comparison, was a commercially available polymer obtained from Kuraray Co. Ltd.

**NMR Measurements.**  $^{13}\text{C}$  NMR spectra were obtained at 125 and 25 MHz by using JEOL GX-500 and JEOL PS-100 high-resolution spectrometers, respectively. The latter was used for the preliminary experiment to determine the optimum parameters for recording the 125-MHz  $^{13}\text{C}$  NMR spectra. Measurements were done in solutions of perdeuterated dimethyl sulfoxide ( $\text{Me}_2\text{SO}-d_6$ , Merck) at  $65^\circ\text{C}$  with a sample concentration of 7 wt % in  $\text{Me}_2\text{SO}-d_6$ .

The 25-MHz  $^{13}\text{C}$  NMR spectra were measured for determining the chemical shifts with respect to internal tetramethylsilane and the spin-lattice relaxation times ( $T_1$ ) for the different types of carbons. The operating conditions were as follows: pulse angle,  $90^\circ$  (pulse width, ca. 20  $\mu\text{s}$ ); pulse repetition time, 8 s; spectral width, 5000 Hz; 4096 data points for Fourier transform (FT); accumulation, 1000 scans; sample tube outside diameter, 8 mm. According to our  $T_1$  measurements, the above pulse repetition time was chosen to be more than five times the longest  $T_1$  value ( $1.44 \pm 0.03$  s) for the carbon of the carbonyl group. The  $T_1$  values at 25 MHz were  $80.4 (\pm 2.5)$  ms and  $1.13 (\pm 0.02)$  s for methine and cyanide carbons, respectively. In order to determine the chemical shifts of methylene carbons, so-called water-eliminated Fourier transform (WEFT) measurements were carried out in order to avoid the overlapping between the signals of the methylene and  $\text{Me}_2\text{SO}-d_6$  carbons. The corresponding pulse sequence was 40  $\mu\text{s}$  ( $180^\circ$ )–0.2 s–20  $\mu\text{s}$  ( $90^\circ$ )–8 s.

The 125-MHz  $^{13}\text{C}$  NMR spectra used in this experiment could provide all the quantitative results concerning monomer sequence distributions and stereochemical configuration. The sample glass tube used at 125 MHz was of 10-mm diameter. The sweep width in the FT mode amounted to 25 000 Hz and the corresponding data points were 16 000. A pulse angle of  $45^\circ$  and a pulse repetition time of 10 s were chosen. The validity of the above repetition time at 125 MHz was confirmed by the fact that the relative intensities for the configurationally different peaks in cyanide carbon resonance were identical at 25 MHz and 125 MHz. Spectra were obtained after accumulation of 4000 scans. The peaks intensities were measured by the cutting and weighing method.

When quantitative NMR measurements were performed, it was considered that the spin-lattice relaxation times were the same for different compositional and configurational sequences. For purposes of comparison, monomer compositions were also obtained from 25-MHz spectra by comparing the peak intensities between carbonyl and cyanide carbons, assuming the same nuclear Overhauser enhancement (NOE) factor between different non-protonated carbons and employing a sufficiently long pulse delay to allow for the  $T_1$  value of the carbonyl carbon.

**Table I**  
**Chemical Shift Assignments and Their Relative Intensities for the Compositional Triad Distributions of Vinylidene Cyanide and Vinyl Acetate Copolymer**

carbon	chemical shift <sup>a</sup>	assignment	relative intensity	
			obsd <sup>b</sup>	calcd
$\text{C}\equiv\text{N}$	115.2 (B), 114.8 (A), 114.3 (B') <sup>c</sup>	(VAc-VDCN-VAc)	0.89	0.889
	113.5, 113.1	(VAc-VDCN-VDCN)	0.10	0.110
	113.3	(VDCN-VDCN-VDCN)	0.01	0.004
		(VDCN-VAc-VDCN)		
CH	65.9, 65.7, 65.5	(VDCN-VAc-VDCN)		
$\text{CH}_2$	40.8	(VAc-VDCN)		
$\text{CH}_3$	21.5, 21.1	(VDCN-VAc-VDCN)	0.82	0.792
	20.1	(VAc-VAc-VDCN)	0.15	0.196
	19.7	(VAc-VAc-VAc)	0.03	0.012

<sup>a</sup> Chemical shift is given with respect to internal tetramethylsilane. <sup>b</sup> Each observed relative value normalized to unity within the error of  $\pm 0.05$ . <sup>c</sup> See Figure 2.

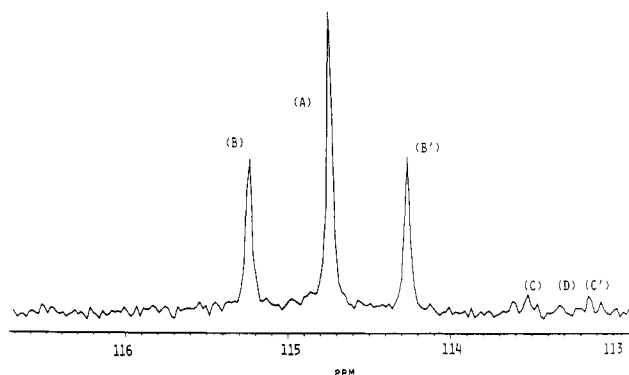


**Figure 2.** Expanded spectrum of the cyanide carbon region of Figure 1.

## Results and Discussion

Figure 1 shows the 125-MHz  $^{13}\text{C}$  NMR spectrum of P(VDCN-VAc) in  $\text{Me}_2\text{SO}-d_6$  solution at  $65^\circ\text{C}$ . The assignments of various resonance peaks have been made by comparison with those of poly(vinyl acetate) and other copolymers involving vinyl acetate.<sup>14,15</sup> The spectrum of poly(vinylidene cyanide) could not be obtained because it is very unstable due to chain scission by atmospheric moisture at room temperature.<sup>16</sup> The assignments are summarized to Table I and will be discussed in detail. From the result that the spectrum of this copolymer is fairly simple, we may conclude that the monomeric units of VDCN and VAc are almost all arranged in a head-to-tail (HT) fashion. If there were some head-to-head (HH) or tail-to-tail (TT) placements, the corresponding  $^{13}\text{C}$  NMR spectrum would be more complicated.

In order to discuss quantitatively the compositional sequence distributions in the following sections, we denote the monomer sequences and the mole fractions of the two monomers by (VAc) and (VDCN), while those of the three dyads are given by (VAc-VDCN), (VAc-VAc), and (VDCN-VDCN-VDCN). A similar notation is employed for the six possible triads, e.g., (VAc-VAc-VAc), VAc-VAc-VDCN, (VAc-VDCN-VDCN), etc.

**Monomer Sequence Distributions.** Figure 2 shows the expanded resonance for the cyanide carbon region that represents all the possible VDCN-centered triads. These triads appear more than expected for the three compositional VDCN triads, showing the effect both of sequence

**Table II**  
Copolymerization Parameters in the Vinylidene  
Cyanide-Vinyl Acetate System Determined from the  
Resonances of Cyanide and Methyl Carbon Atoms

$r_1$	0.064 ( $\pm 0.006$ ), 0.11 (0.073–0.20) <sup>a</sup>
$r_2$	0.116 ( $\pm 0.006$ ), 0.0054 (0.0026–0.013) <sup>a</sup>
$P_{12}$	0.940 ( $\pm 0.005$ )
$P_{21}$	0.895 ( $\pm 0.005$ )
$\bar{N}_1$	1.064 ( $\pm 0.006$ )
$\bar{N}_2$	1.116 ( $\pm 0.006$ )

<sup>a</sup> Data from the copolymerization equation (ref 18).

distribution and configurational effects. With respect to the compositional triads, the cyanide carbon resonances in Figure 2 are classified into (A, B, B'), (C, C'), and (D), corresponding to the VDCN-centered triads of (VAc-VDCN-VAc), (VAc-VDCN-VDCN), and (VDCN-VDCN-VDCN), respectively. Splitting into A, B, and B' or C and C' is considered to originate from the configurational effects that will be discussed in the next section. Apparently, the alternating triad (VAc-VDCN-VAc) is remarkably dominant while the VDCN homotriad is almost negligible. This negligible composition of the content of VDCN homotriad may be due to the chain scission in VDCN homosequence that results in an addition of VAc unit to the VDCN chain end.

Now we consider the copolymerization mechanism. From the compositional results with respect to the VDCN-centered triads, the conditional probability  $P_{12}$ , representing that a growing chain ending of VDCN unit will add a VAc unit to give a sequence of VDCN-VAc, can be obtained.

$$P_{12} = [(VAc-VDCN-VAc) + (VAc-VDCN-VDCN)/2] / [(VAc-VDCN-VAc) + (VAc-VDCN-VDCN) + (VDCN-VDCN-VDCN)] \quad (1)$$

Thus the number-average sequence length of VDCN,  $\bar{N}_1$ , being the reciprocal of  $P_{12}$ , can be easily calculated. The VDCN-reactivity ratio  $r_1$  can be theoretically calculated by introducing  $P_{12}$  (or  $\bar{N}_1$ ) into the relationship

$$r_1 = \frac{[M_2]}{[M_1]} \left( \frac{1}{P_{12}} - 1 \right) = \frac{[M_2]}{[M_1]} (\bar{N}_1 - 1) \quad (2)$$

where  $[M_1]$  and  $[M_2]$ , representing the respective mole fractions of VDCN and VAc monomer feeds in the reactant mixture, are equal to a value of 0.5. The ratio of  $[M_1]/[M_2]$  being unity is unchanged throughout the whole copolymerization process due to an alternating character. We can therefore determine  $r_1$  reasonably from eq 2. The advantage of the usage of NMR in the determination of monomer reactivity ratios is in the requirement of data from only one copolymer.<sup>17</sup> The calculated values of  $P_{12}$ ,  $\bar{N}_1$ , and  $r_1$  are given in Table II. As expected, all of these parameters show that VAc monomer is preferentially added to the growing chain end of VDCN units in the propagation reaction.

In contrast, compositional information concerning the VAc-centered triads can be obtained from the methyl resonance. As seen in Figure 3, the resonance of the methyl carbons is split into three main peaks due to the VAc-centered triads that are assigned to (VDCN-VAc-VDCN), (VAc-VAc-VDCN), and (VAc-VAc-VAc) from low to high field. This assignment has been made on the basis of the chemical shift of the methyl carbon resonances for poly(vinyl acetate) in  $Me_2SO-d_6$ . Likewise with VDCN-centered triads, the (VDCN-VAc-VDCN) triad is dominant to an extent of more than 80% among the VAc-centered triads. In the resonance region corresponding to

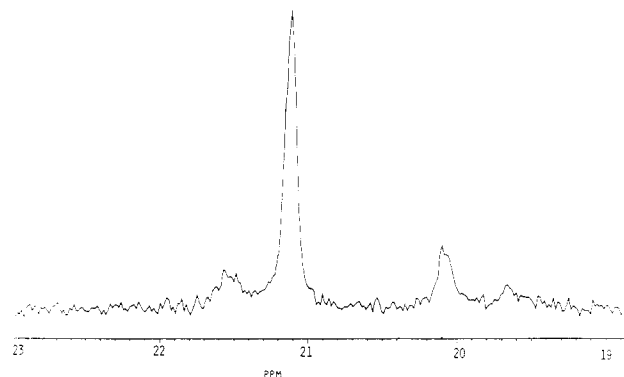


**Figure 3.** Expanded spectrum of the methyl carbon region of Figure 1.

(VDCN-VAc-VDCN) triads, the weak peak appearing at lower field is due to nonalternating pentads, whereas the main peak at 21.08 ppm represents the alternating VAc-centered pentad.

In the same manner as in the case of VDCN-centered triads, copolymerization parameters with respect to the VAc monomer unit can be determined directly from the compositional distributions of VAc-centered triads by using the relationships

$$P_{21} = [(VDCN-VAc-VDCN) + (VAc-VAc-VDCN)/2] / [(VDCN-VAc-VDCN) + (VAc-VAc-VDCN) + (VAc-VAc-VAc)] \quad (3)$$

$$r_2 = \frac{[M_1]}{[M_2]} \left( \frac{1}{P_{21}} - 1 \right) = \frac{[M_1]}{[M_2]} (\bar{N}_2 - 1) \quad (4)$$

These parameters are given together with those for the VDCN unit in Table II, where the small values of both  $r_1$  and  $r_2$  provide a certain proof that P(VDCN-VAc) is an almost alternating copolymer. The reactivity ratios determined by Gilbert et al.<sup>18</sup> using the Mayo-Lewis copolymerization equation, are also listed in Table II. The reactivity ratios from our NMR analysis and the copolymerization equation show the strong tendency of VDCN and VAc to alternate during copolymerization. From our results, it is considered that the reactivity of VAc toward the VDCN free radical is greater than that of VDCN toward the VAc free radical, while the conclusions of Gilbert et al. are opposite to ours. Supporting our results, it was observed that for the acrylonitrile-vinyl acetate copolymer the tendency to form an alternating structure was most pronounced only in the presence of excess VAc.<sup>15</sup>

As one of the main purposes in the present study, monomer compositions of VDCN and VAc are determined by using the above compositional distributions of VDCN- and VAc-centered triads. These six possible triads make it possible to give the calculated compositions for the three dyads, i.e., (VDCN-VDCN), (VAc-VAc), and (VAc-VDCN). The compositions of (VDCN-VDCN) and (VAc-VAc) can be calculated from the resonances of cyanide and methyl carbon atoms, respectively, as follows:

$$(VDCN-VDCN) = \frac{(VDCN-VDCN-VDCN) + (VAc-VDCN-VDCN)/2}{(VDCN-VDCN-VDCN) + (VAc-VDCN-VDCN)/2 + (VAc-VAc-VDCN)/2} \quad (5a)$$

$$(VAc-VAc) = \frac{(VAc-VAc-VAc) + (VAc-VAc-VDCN)/2}{(VAc-VAc-VAc) + (VAc-VAc-VDCN)/2 + (VAc-VAc-VDCN)/2} \quad (5b)$$

Numerical values of the above two were 0.06 and 0.11, respectively, for the copolymer. Thus, the composition of the (VAc-VDCN) dyad becomes 0.83. In principle, the

**Table III**  
Theoretical Mole Fractions of All the Possible Triads in Vinylidene Cyanide-Vinyl Acetate Copolymer

triad	equation <sup>a</sup>	triad fraction
(VAc-VAc-VAc)	$(VAc)(1 - P_{21})^2$	0.006
(VAc-VAc-VDCN)	$(VAc)(1 - P_{21})P_{21} + (VDCN)P_{12}(1 - P_{21})$	0.096
(VDCN-VAc-VDCN)	$(VDCN)P_{12}P_{21}$	0.400
(VDCN-VDCN-VDCN)	$(VDCN)(1 - P_{12})^2$	0.002
(VAc-VDCN-VDCN)	$(VDCN)(1 - P_{12})P_{12} + (VAc)P_{21}(1 - P_{12})$	0.055
(VAc-VDCN-VAc)	$(VAc)P_{21}P_{12}$	0.442

<sup>a</sup> Based upon the following parameters: (VAc) = 0.525, (VDCN) = 0.475,  $P_{12}$  = 0.940, and  $P_{21}$  = 0.895.

resonance of the methylene carbons also provides the same information directly but was unavailable due to overlapping with  $Me_2SO-d_6$  peaks. Consequently, monomer compositions of (VAc) and (VDCN) are easily calculated from the dyad compositions in a similar way:

$$(VDCN) = (VDCN-VDCN) + (VAc-VDCN)/2 \quad (6a)$$

$$(VAc) = (VAc-VAc) + (VAc-VDCN)/2 \quad (6b)$$

Numerical values of these two were 0.475 and 0.525, respectively. The monomer compositions determined from the peak intensities measured at 25 MHz between carbonyl and cyanide carbon atoms are 0.45<sub>4</sub> for (VDCN) and 0.54<sub>6</sub> for (VAc), showing a good agreement with the above-calculated compositions. This result clarifies the smaller  $r_1$  compared with  $r_2$ .

To provide more quantitative information on these compositional distributions, we calculated the theoretical compositions for all six triads, using the monomer compositions of VDCN and VAc as well as the conditional probabilities for cross propagation  $P_{12}$  and  $P_{21}$ :

$$(VAc-VDCN-VAc) = (VAc)P_{21}P_{12} \quad (7a)$$

and

$$(VAc-VAc-VDCN) = (VAc)(1 - P_{21})P_{21} + (VDCN)P_{12}(1 - P_{21}) \quad (7b)$$

Numerical values are 0.442 and 0.096, respectively. The other triad compositions are calculated in similar ways, as shown in Table III. The validity of this approach can be confirmed by the fact that the total sum of the theoretical compositions for all the possible compositional triads is equal to unity, although these compositions were obtained by using the independently determined  $P_{12}$  and  $P_{21}$ .

Furthermore, the data of the six triad compositions determined theoretically make it possible to derive the calculated relative intensities with respect to VDCN- and VAc-centered triads separately; these are given in Table I alongside the observed values. The agreement between the observed and the calculated values is satisfactory, especially in the resonance region of cyanide carbon atoms.

In contrast, quantitative analysis could not be done regarding methylene carbon resonances which have been deemed most available to understand the dyad-compositional distributions. As seen in Figure 4, the methylene carbon resonances are overlapped partially with  $Me_2SO-d_6$  peaks. However, only a single resonance signal related to (VAc-VDCN) was observed at 40.8 ppm in the WEFT measurement at 25 MHz, while the methylene carbon resonance related to the (VAc-VAc) dyad has been known to be at 38.4 ppm. This also supports our conclusion that P(VDCN-VAc) is an alternating copolymer.

**Configuration in the Alternating Sequence.** As discussed in the preceding section, we know that P(VDC-

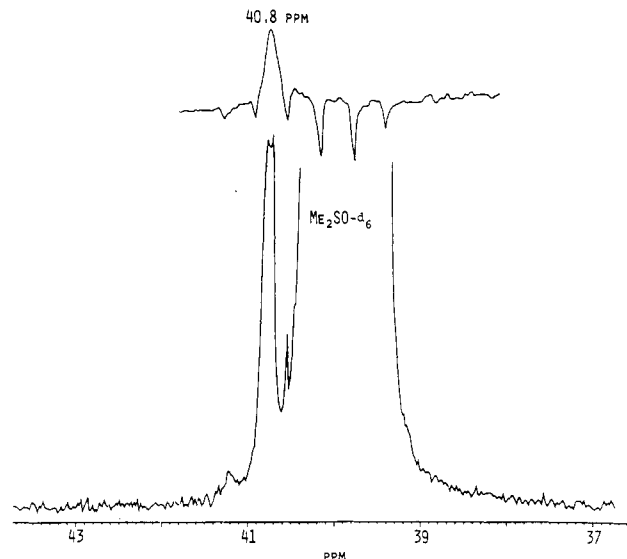
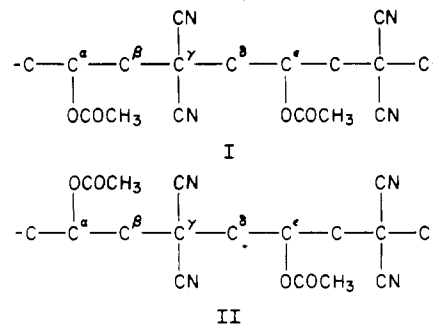
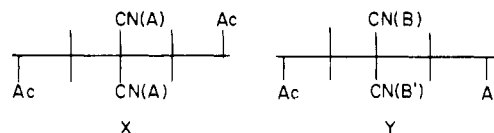


**Figure 4.** Expanded spectrum of methylene carbon region of Figure 1. The upper spectrum represents the WEFT  $^{13}C$  NMR spectrum of methylene carbon at 25 MHz, indicating the absence of the fraction of methylene resonance in the resonance of  $Me_2SO-d_6$ .

N-VAc) is an alternating copolymer in a head-to-tail arrangement with a (VAc-VDCN) dyad composition of 0.83. For the alternating sequence with VAc and VDCN units, only the VAc unit shows a configurational feature because the VDCN unit contains no asymmetric carbon. Considering the VAc-VDCN unit as a repeating unit in the alternating copolymer, two configurationally different structures in dyad sense are possible, I and II. Formulas



I and II represent segments of the copolymer chain. Here, we define the configurations in I and II as  $\epsilon$ -isotactic and  $\epsilon$ -syndiotactic, respectively, with respect to the acetate substituents attached to  $C^a$  and  $C^c$  carbons.<sup>19</sup> The relative configurational enchainment in I is defined as  $m_\epsilon$  ( $\epsilon$ -meso), whereas that in II is defined as  $r_\epsilon$  ( $\epsilon$ -racemo). The 125-MHz  $^{13}C$  NMR spectrum provides this  $\epsilon$ -tactic information. As described earlier in Figure 2, splitting of cyanide carbon resonance into three peaks, A, B, and B', related to the (VAc-VDCN-VAc) triad is caused by the  $\epsilon$ -relative enchainment. In respect to the configurational sequence, the (VAc-VDCN-VAc) triad exists in two types:



According to the designation of  $\epsilon$ -tacticity, VDCN-centered triads of X and Y types are  $\epsilon$ -syndiotactic ( $r_\epsilon$ ) and  $\epsilon$ -isotactic ( $m_\epsilon$ ), respectively. Thus, the cyanide carbon resonances show resolution of three peaks corresponding to the three magnetically nonequivalent carbons of A, B, and B'.

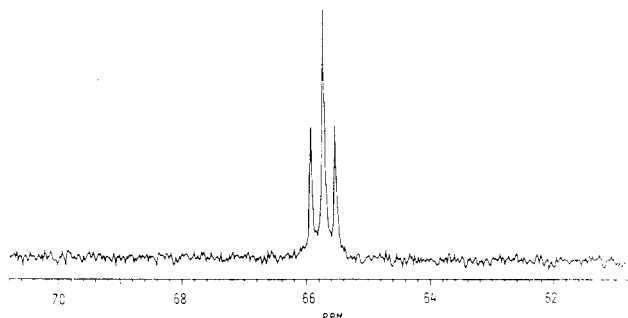


Figure 5. Expanded spectrum of the methine carbon region of Figure 1.

Although the assignment between B and B' carbons is not clearly verified, it is considered that resonance of carbon B' appears at higher field region than that of carbon B due to the C=O bond anisotropy and/or the anisotropy of the electron density, which may be similar to the case of styrene-methyl methacrylate copolymer where the coisotactic peak has been assigned at higher field compared with the cosyndiotactic one.<sup>20,21</sup> Apparently the peak at intermediate field is assigned as resonance of carbon A. The  $\epsilon$ -isotacticity  $\sigma_\epsilon$  is easily obtained from these peak intensities from the relationship

$$\sigma_\epsilon = \frac{[Y]}{[X] + [Y]} = \frac{[B] + [B']}{[A] + [B] + [B']} \quad (8)$$

where [X] and [Y] represent the respective compositions of  $\epsilon$ -syndiotactic and  $\epsilon$ -isotactic triads and [A], [B], and [B'] are the relative intensities of the corresponding cyanide carbon resonances. When the data are introduced that the peak intensity ratio of the above spatially different cyanide carbons is 2.00(A):1.04(B):1.00(B'), the calculated  $\sigma_\epsilon$  value of 0.506 is obtained from eq 8. Equal population is, therefore, suggested between X and Y triads. It means a nonstereoregular structure in an alternating copolymer. Probably, because of the absence of the stereoregularity of a VAc unit with the nearest-neighbor one, any ordered structure in P(VDCN-VAc) has never been observed in X-ray diffraction or DSC thermogram.

In Figure 5, the methine carbon resonances at 125 MHz are also split into three peaks due to the configurational pentad distributions. Taking into account VAc-VDCN as a repeating unit in the alternating copolymer, the three peaks due to methine carbon atom have been considered for  $\epsilon$ -tactic triads, with  $\epsilon$ -syndiotactic ( $r,r_\epsilon$ ),  $\epsilon$ -heterotactic ( $m,r_\epsilon + r,m_\epsilon$ ), and  $\epsilon$ -isotactic ( $m,m_\epsilon$ ) from low to high field. Although the assignment for  $\epsilon$ -syndiotactic and  $\epsilon$ -isotactic triads is not fully clarified, our tentative assignment provides the value of  $\sigma_\epsilon$  determined from methine carbon resonances in fairly good agreement with that from cyanide carbon resonances. Their  $\epsilon$ -tactic probability ratio is expected to be  $(1 - \sigma_\epsilon)^2 : 2\sigma_\epsilon(1 - \sigma_\epsilon) : \sigma_\epsilon^2$ , if one assumes a terminal Bernoullian control with single parameter  $\sigma_\epsilon$ .<sup>22</sup> When  $\sigma_\epsilon$  of 0.506 determined by cyanide carbon resonances is used, this probability is calculated as 0.244:0.500:0.256, which agrees well with the observed ratio (0.24:0.50:0.26). The resonances for nonalternating VAc-centered triads involving (VAc-VAc-VDCN) and (VAc-VAc-VAc) are not observed separately. The expected resonance pattern for (VAc-VAc-VDCN) is considered to be a doublet with equal intensity and must be overlapped symmetrically with a  $\epsilon$ -heterotactic peak of (VDCN-VAc-VDCN) triad.

Also for the methylene carbon resonances, this configurational feature can be observed in a way that the peaks corresponding with the (VAc-VDCN) dyad are finely split

into a doublet, as seen in Figure 4. The doublet peaks representing different  $\epsilon$ -tactic dyads are of nearly equal intensities, supporting our conclusion that P(VDCN-VAc) has a nonstereoregular structure (i.e.,  $\sigma_\epsilon \approx 0.5$ ).

In contrast, analogous to the case of poly(vinyl acetate), the carbonyl carbon resonance of P(VDCN-VAc) shows a sharp peak. Thus carbonyl carbon atoms of both P(VDCN-VAc) and poly(vinyl acetate) are considered to be insensitive to the configurational effect.

## Conclusion

The  $^{13}\text{C}$  NMR spectrum gives detailed information such that P(VDCN-VAc) is an alternating copolymer in a HT arrangement and has a nonstereoregular structure. Due to this nonstereoregularity, P(VDCN-VAc) is considered to be amorphous, and this has been investigated by X-ray diffraction and DSC measurements. Presumably, significant piezoelectricity in P(VDCN-VAc) can be explained by the alternating sequence of the chain microstructure. Under poling at high dc electric field, the VAc unit located between VDCN is thought to facilitate the rotation of main chains, which ultimately causes the dipole orientation of cyanide group. Even if poly(vinylidene cyanide) were available in a film state, it would be difficult to rotate main chains because of a strong dipolar interaction between cyanide groups. To design a new piezoelectric copolymer having a large dipole moment of cyanide group, it would be essential to find an active comonomer with a vinylidene cyanide monomer forming an alternating copolymer, and we should take into account the  $\epsilon$ -configurational effect in analyzing its corresponding  $^{13}\text{C}$  NMR spectrum.

**Acknowledgment.** We thank Dr. S. Amiya of central research laboratories, Kuraray Co. Ltd, Japan, for recording the 125-MHz  $^{13}\text{C}$  NMR spectrum. Y.S.J. wishes also to thank Sunkyoung Fibres Ltd., Korea, for granting his leave of absence.

## References and Notes

- (1) Lovinger, A. J. In "Developments in Crystalline Polymer, 1"; Bassett, D. C., Ed.; Applied Science: London, 1982.
- (2) Hasegawa, R.; Takahashi, Y.; Tadokoro, H. *Polym. J.* **1972**, *3*, 600.
- (3) Lovinger, A. J.; Davis, G. T.; Furukawa, T.; Broadhurst, M. G. *Macromolecules* **1982**, *15*, 323.
- (4) Davis, G. T.; Furukawa, T.; Lovinger, A. J.; Broadhurst, M. G. *Macromolecules* **1982**, *15*, 329.
- (5) Miyata, S.; Yoshikawa, M.; Tasaka, S.; Ko, M. *Polym. J.* **1980**, *12*, 857.
- (6) Tasaka, S.; Miyasato, K.; Yoshikawa, M.; Miyata, S.; Ko, M. *Ferroelectrics* **1984**, *57*, 267.
- (7) Jo, Y. S.; Tasaka, S.; Miyata, S. *Sen-i Gakkaishi* **1983**, *39*, 451.
- (8) Marshall, A. S.; Petrie, S. E. B. *J. Appl. Phys.* **1975**, *46*, 4223.
- (9) Douglass, D. C.; McBrierty, V. J.; Wang, T. T. *J. Chem. Phys.* **1982**, *77*, 5826.
- (10) McBrierty, V. J.; Douglass, D. C.; Wang, T. T. *Appl. Phys. Lett.* **1982**, *41*, 1051.
- (11) Bovey, F. A. *Prog. Polym. Sci.* **1971**, *3*, 1.
- (12) Sohma, J.; Chûjô, R. In "Magnetic Resonance in High Polymers"; Kyoritsu Shuppan: Tokyo, 1975.
- (13) Ardis, A. E.; Averill, S. J.; Gilbert, H.; Miller, F. F.; Schmidt, R. F.; Stewart, F. D.; Trumbull, H. L. *J. Am. Chem. Soc.* **1950**, *72*, 1305.
- (14) van der Velden, G.; Beoulen, J. *Macromolecules* **1982**, *15*, 1071.
- (15) Kalyanam, N.; Gandhi, V. G.; Sivaram, S.; Bhardwaj, I. S. *Macromolecules* **1982**, *15*, 1636.
- (16) Gilbert, H.; Miller, F. F.; Averill, S. J.; Schmidt, R. F.; Stewart, F. D.; Trumbull, H. L. *J. Am. Chem. Soc.* **1954**, *76*, 1074.
- (17) Chûjô, R. *J. Phys. Soc. Jpn.* **1966**, *21*, 2669.
- (18) Gilbert, H.; Miller, F. F.; Averill, S. J.; Carlson, E. J.; Folt, V. L.; Heller, H. J.; Stewart, F. D.; Schmidt, R. F.; Trumbull, H. L. *J. Am. Chem. Soc.* **1956**, *78*, 1669.
- (19) Greek alphabet is used to designate the separation of two skeletal carbons attached to the groups under consideration. According to this terminology, tactic structure of polymers may be defined more easily and generally. For example, the

dyad configurations of poly(propyl oxide) are termed as  $\delta$ -meso and  $\delta$ -racemo for dyad tactic structures. By the same way, those of polypropylene are termed as  $\gamma$ -meso and  $\gamma$ -racemo.

(20) Hirai, H.; Koinuma, H.; Tanabe, T.; Takeuchi, K. *J. Polym. Sci., Polym. Chem. Ed.* **1979**, *17*, 1339.

(21) Ebdon, J. R.; Huckerby, T. N.; Khan, I. *Polym. Commun.* **1983**, *24*, 162.

(22) Bovey, F. A.; Tiers, G. V. D. *J. Polym. Sci.* **1960**, *44*, 173.

## Confined-Chain Statistics of Block Polymers and Estimation of Optical Anisotropy and Domain Size

Takeji Hashimoto,\* Mitsuhiro Shibayama,<sup>†</sup> and Hiromichi Kawai<sup>‡</sup>

Department of Polymer Chemistry, Faculty of Engineering, Kyoto University, Kyoto 606, Japan

Dale J. Meier\*

Michigan Molecular Institute, Midland, Michigan 48640. Received December 7, 1984

**ABSTRACT:** Optical anisotropy of block polymer chains in lamellar microdomains has been calculated on the basis of a modified confined-chain statistics. The results show that the anisotropy associated with molecular orientation is an order of magnitude smaller than that associated with form anisotropy for polystyrene-polyisoprene and polystyrene-polybutadiene A-B type diblock and A-B-A type triblock polymers. Compared with the statistics originally proposed by one of us (D.J.M.), the modification involves elimination of the narrow-interphase approximation and use of a different functional form for the segmental density distribution across the interface. The modification is shown to give a better agreement with the experimental results.

### I. Introduction

A-B and A-B-A type di- and triblock polymers form microdomain structure as a consequence of microphase separation of constituent block chains A and B under the strong segregation limit where they have a strong repulsive interaction. In this paper we will estimate the "intrinsic" optical anisotropy of block polymers forming lamellar microdomains, a special type of the microdomain morphology that is formed when the molecular volume of A (in the case of A-B diblock polymers) or of 2A (in the case of A-B-A triblock block polymers) is about equal to that of B.

We will restrict our treatment here to the case where both A and B are amorphous. The estimation of the intrinsic optical anisotropy involves the calculation of both molecular anisotropy and form anisotropy. The molecular anisotropy is the anisotropy due to molecular orientation of A and B chains in the domain space. The chemical junction points between A and B are localized somewhere in the interface, and the end-to-end vectors of A and B chains are statistically oriented normal to the interface. In this paper we will estimate this anisotropy based on an approximate method that involves two steps: (i) first we calculate the mean-square end-to-end distance of each block chain parallel ( $\langle r^2 \rangle$ ) and perpendicular ( $\langle (z - z')^2 \rangle$ ) to the interface on the basis of the "confined-chain statistics" proposed by one of us<sup>1-3</sup> and then (ii) knowing the results of (i), we calculate the orientational anisotropy of the chains based upon the Kuhn-Grün theory.<sup>4,5</sup> The Kuhn-Grün theory, which interrelates the anisotropy of a chain with its end-to-end displacement, is valid for the chains in free space but not for the block chains A and B in the confined space. Thus the second step involves an approximation, as will be discussed in section II-2.

The form anisotropy is the anisotropy arising from the distortion of the electric field strength of the incident light wave at the phase boundaries between the two coexisting phases<sup>6</sup> when there is a difference in their refractive indices. The greater the difference of the refractive indices and the greater the asymmetry in the shape of each phase, the larger is the form anisotropy. The form anisotropy (birefringence) was studied by Wiener<sup>6</sup> for two-phase systems in which each phase is optically isotropic and the boundary between the two phases is sharp, with the refractive index varying stepwise across the interface. Thus the estimation of the form anisotropy for the block polymer systems involves generalization of the theory to account for the finite thickness of the domain boundary region as well as for molecular anisotropy (see section III).

### II. Molecular Anisotropy of Block Polymer Chains in the Domain Space

Let us take a reference axis  $z$  perpendicular to the interfaces between A and B lamellar domains. The A and B chains in the A-B diblock polymer are joined somewhere in the interface (chemical junction), and all their segments are restricted in the A and B domains (Figure 1a). Their end-to-end vectors orient uniaxially with respect to the reference axis.

The molecular anisotropy of the  $j$ th chain in A domain with its end-to-end vector  $\mathbf{R}_j$  oriented at the polar angle  $\theta_j$  with respect to the  $z$  axis is given by

$$P_{1j} - P_{2j} = (\pi_{1j} - \pi_{2j})(3 \cos^2 \theta_j - 1)/2 \quad (\text{II-1})$$

where  $P_{1j}$  and  $P_{2j}$  are the polarizabilities of a single chain parallel and perpendicular to  $z$ , respectively, and  $\pi_{1j}$  and  $\pi_{2j}$  are the polarizabilities parallel and perpendicular to the end-to-end vector  $\mathbf{R}_j$  (Figure 1b).

**1. Application of Kuhn-Grün Statistics for the Confined Chains.** The molecular anisotropy of the single chain A in the confined space, in turn, may be approximately given by Kuhn-Grün chain statistics.

$$\pi_{1j} - \pi_{2j} = \sigma_A(b_1 - b_2)A_f^s \quad (\text{II-2})$$

<sup>†</sup> Present address: Department of Polymer Science and Engineering, Kyoto Institute of Technology, Matsugasaki, Sakyo-ku, Kyoto 606, Japan.

<sup>‡</sup> Present address: Hyogo University of Education, Hyogo-ken 673-14, Japan.